This is a repository copy of *Acceleration of M-S-H gel formation through the addition of alkali carbonates*.

White Rose Research Online URL for this paper:
http://eprints.whiterose.ac.uk/149610/

Version: Accepted Version

Proceedings Paper:
Zhao, H., Hanein, T. orcid.org/0000-0002-3009-703X, Li, N. et al. (4 more authors) (2019) Acceleration of M-S-H gel formation through the addition of alkali carbonates. In: Proceedings of the 15th International Congress on the Chemistry of Cement (ICCC 2019). 15th International Congress on the Chemistry of Cement, 16-20 Sep 2019, Prague, Czech Republic. .

Reuse
Items deposited in White Rose Research Online are protected by copyright, with all rights reserved unless indicated otherwise. They may be downloaded and/or printed for private study, or other acts as permitted by national copyright laws. The publisher or other rights holders may allow further reproduction and re-use of the full text version. This is indicated by the licence information on the White Rose Research Online record for the item.

Takedown
If you consider content in White Rose Research Online to be in breach of UK law, please notify us by emailing eprints@whiterose.ac.uk including the URL of the record and the reason for the withdrawal request.

eprints@whiterose.ac.uk
https://eprints.whiterose.ac.uk/

Acceleration of M-S-H gel formation through the addition of alkali carbonates

Han Zhao[a], Theodore Hanein[b], Nabaichuan Li[c], Abdullah Alotaibi[d], Ang Li[e], Samuel Walling[f], Hajime Kinoshita[g]

Materials Science & Engineering, The University of Sheffield, Sheffield, United Kingdom

[a]HZhao21@sheffield.ac.uk
[b]t.hanein@sheffield.ac.uk
[c]nli9@sheffield.ac.uk
[d]aalotaibi3@sheffield.ac.uk
[e]ALi7@sheffield.ac.uk
[f]s.walling@sheffield.ac.uk
[g]h.kinoshita@sheffield.ac.uk

ABSTRACT

The varied properties of different cements enable the cement industry to shift towards the manufacture of application-specific cements rather than a general-purpose binder. M-S-H cements could offer a good alternative for specialist application, and could potentially have a lower carbon footprint as they require much lower temperatures for their production compared with Portland cement (PC). M-S-H cements harden with M-S-H gel as a binding phase, which is the equivalent of calcium silicate hydrate (C-S-H) gel in PC. However, the development of M-S-H is much slower than that of C-S-H, resulting in insufficient strength development of the product; thus, limiting the applications of M-S-H cement. The present study investigates the effects of an additive to enhance the development of M-S-H gel. Sodium bicarbonate was tested, and its impacts on the evolution of M-S-H gel were studied. The obtained results indicate that sodium bicarbonate has the ability to aid the development of M-S-H by promoting the reaction of Mg(OH)2 and SiO2, which resulted in the accelerated development of M-S-H gel.

Acceleration of M-S-H gel formation through the addition of alkali carbonates

Han Zhao, Theodore Hanein, Nabaichuan Li, Ang Li, Abdullah Alotaibi, Samuel Walling and Hajime Kinoshita*

Department of Materials Science and Engineering, the University of Sheffield, Sheffield S1 3JD, UK

Abstract (250 words max)

The varied properties of different cements enable the cement industry to shift towards the manufacture of application-specific cements rather than a general-purpose binder. M-S-H cements could offer a good alternative for specialist application, and could potentially have a lower carbon footprint as they require much lower temperatures for their production compared with Portland cement (PC). M-S-H cements harden with M-S-H gel as a binding phase, which is the equivalent of calcium silicate hydrate (C-S-H) gel in PC. However, the development of M-S-H is much slower than that of C-S-H, resulting in insufficient strength development of the product; thus, limiting the applications of M-S-H cement. The present study investigates the effects of an additive to enhance the development of M-S-H gel. Sodium bicarbonate was tested, and its impacts on the evolution of M-S-H gel were studied. The obtained results indicate that sodium bicarbonate has the ability to aid the development of M-S-H by promoting the reaction of $Mg(OH)_2$ and SiO_2, which resulted in the accelerated development of M-S-H gel.

* Corresponding author: h.kinoshita@sheffield.ac.uk

1. INTRODUCTION

1.1 Background

Magnesia-based cements are generally produced from a mixture of magnesium oxide MgO (or hydroxide $Mg(OH)_2$) and reactive silica SiO_2 (e.g. silica fume). Upon reaction with water, the system forms magnesium silicate hydrate (M-S-H) gel as a "binding" phase, which is the equivalent of calcium silicate hydrate (C-S-H) gel in Portland cement.

One of the key challenges for wider application of magnesia-based cements is obtaining the raw material MgO or $Mg(OH)_2$. Although MgO has a much lower firing temperature (~650 ℃), compared with the generally employed Portland cement, for its production from $MgCO_3$ in conventional kilns (Taylor & Collins 2006), it is still carbon-intensive because ~52 wt.% of $MgCO_3$ is CO_2 and the reaction is endothermic. $MgCO_3$ is also scarce itself. Further developing carbon-efficient technologies to extract MgO or $Mg(OH)_2$ from these rocks would help to establish magnesia-based eco-cements (Gartner & Sui 2018).

Magnesia-based cements can still have a great potential to be used for specialist application, for example, encapsulation of nuclear wastes such as Magnox sludge (Walling et al. 2015), where the embodied magnesium oxide in the waste can be directly utilised together with reactive silica to form the hardened M-S-H cement matrix; thus, encapsulating the radioactive components without a need of conventional cement matrix. M-S-H gel is also shown to be an excellent material to stabilise the heavy metals in contaminated sediment (Wang et al. 2018). These ecological benefits of using magnesia-based cements encourage further research in the field.

The application of M-S-H cement is currently restricted by its relatively slow setting time and strength development. Unfortunately, information related to the structure and properties development of M-S-H gel is still limited, as it is a relatively new kind of binder system. Therefore, the present study investigates the effects of additive to in order to enhance the development of M-S-H gel. Sodium bicarbonate is tested, with the positive utilisation of carbonate ions in mind, and their impacts on the evolution of M-S-H gel were studied.

1.2 Formation of M-S-H gel

M-S-H is typically formed by the reaction between magnesium oxide, reactive silica (e.g. silica fume), and water: $MgO + mSiO_2 + nH_2O \rightarrow MgO \cdot mSiO_2 \cdot nH_2O$ (Nied et al. 2016). The reaction of MgO with a soluble source of silica at room temperature generally forms a gel with a varying Mg/Si ratio (Li et al. 2014, Nied et al. 2016, Walling & Provis 2016, Wang et al. 2018).

It is known that the pH of the reaction solution can affect the formation of M-S-H gels. The pH of a saturated $Mg(OH)_2$ solution is approximately 11, and the solubility of $Mg(OH)_2$ increases when the pH value is below 11 (Figure 1). This is expected because the solubility of Mg^{2+} ions follows the solubility product constant of $[Mg^{2+}][OH^-]^2$, thus, the solubility of Mg^{2+} ions decreases with increasing alkalinity of the mixture. This implies that lower pH is favourable in terms of Mg contribution to M-S-H formation, as a high Mg^{2+} concentration promotes the formation rate of M-S-H (Li et al. 2014). The solubility of the silica also affects the formation of M-S-H, and the rate of formation is depressed when the concentration of silicate in the solution is not sufficient. The solubility of the silica depends on the concentration of OH^- per unit surface area of silica, and the OH^- ions are able to weaken the bonds between the silicon and oxygen atoms (Iler 1979). The solubility of silica increases from 138 mg/L to 876 mg/L when the pH changes from 9 to 10.6 (Jin & Al-Tabbaa 2013). Therefore, the higher pH is favourable in terms of silica contribution to M-S-H formation.

The reverse change in the solubility of $Mg(OH)_2$ and SiO_2 would lead to a balance point between Mg and Si concentrations available to produce M-S-H gel. The dashed lines in Figure 1 (Nied et al. 2016) represent the solubility of amorphous SiO_2 and brucite. The region of pH ~10 demonstrates a relatively high solubility both for brucite and silica, which suggest that higher pH than neutral pH=7 is more beneficial for M-S-H formation. In the present work, as a preliminary investigation, the initial pH conditions are varied via the addition $NaHCO_3$ to the distilled water used for the reaction.

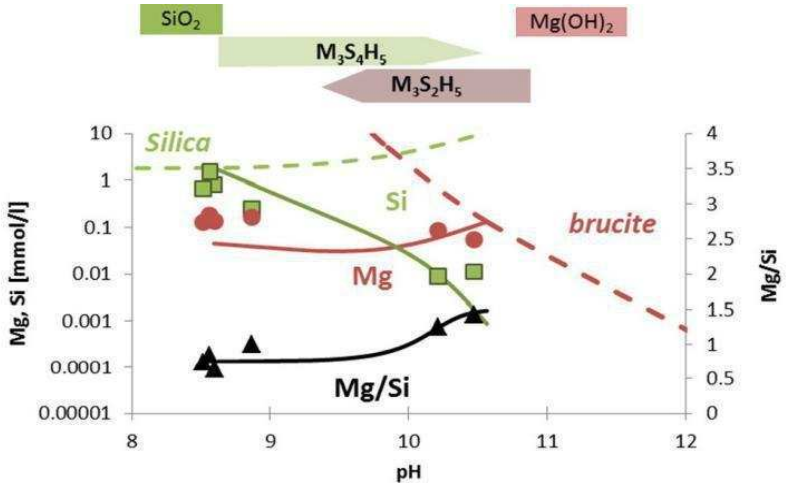

Figure 1. Concentration of Mg and Si in M-S-H at different pH (Nied et al. 2016). Si (■) and Mg (●) concentrations are presented together with Mg/Si ratio (▲). The dashed lines are the solubility of amorphous SiO_2 and brucite.

2. EXPERIMENTAL

2.1 Materials and sample preparation

To study the effect of sodium bicarbonate on the evolution of M-S-H gel, cement pastes were prepared with two different initial water solutions and characterised at different curing times. Samples were prepared by mixing $Mg(OH)_2$ powder with silica fume and one of the solutions as shown in Table 1 for ~10 minutes. 200 mL of distilled water was used to prepare each solution: distilled water and saturated $NaHCO_3$ solution. The amount of $NaHCO_3$ added was set by its solubility at room temperature. The details of the raw materials used are listed in Table 2.

Table 1. Composition and initial pH of solutions for the systems studied

Solution				Solid	
	Water (mL)	**Carbonate (g)**	**pH at 20℃**	**$Mg(OH)_2$ (g)**	**Silica fume (g)**
Distilled water	200	N/A	6.2	100.1	100.0
$NaHCO_3$ solution	200	19.2	8.8	100.1	100.0

Table 2. Information of the materials used

	$Mg(OH)_2$	**Microsilica 940-U**	**$NaHCO_3$**
Supplier	Sigma-Aldrich	Elkem	Sigma-Aldrich
Purity	≧ 95%	90%	≧ 99.0%

Samples were allowed to cure in closed 50 mL centrifuge tubes in an oven at 35°C for 3, 7, 14, 28, 56 and 112 days. The cured samples were then crushed (if hardened) and washed with approximately 100 mL of acetone in order to arrest the hydration reaction. The washed mixture was then recovered from the acetone using filter paper and a vacuum pump assisted Büchner funnel for approximately 30 minutes, after which the solid component was collected. The powder was then dried in a desiccator under vacuum for more than 3 hours and then stored in sealed tubes until characterisation.

2.2 Characterisation

X-ray diffraction (XRD) was used to assess the materials consumption and M-S-H evolution in the different samples. A benchtop Bruker D2 PHASER apparatus armed with a Cu-Kα radiation source running at 30kV and 10mA was used. A one mm divergence slit was used, and the upper and lower discriminators were set at 0.11 and 0.25 V respectively. Diffraction patterns were collected over 5 – 80° 2θ with an increment of 0.02. All samples rotated at 15 rpm during measurements.

X-Ray Fluorescence (XRF) was used to determine oxide composition of the silica fume and the 56 day cured samples for each formulation to check the purity of the microsilica and to determine the amount of sodium remaining in the produced solid after being washed with acetone. A Claisse LeNeo Fluxer was used to make beads, and the XRF measurement was conducted using PANalytical's Zetium operated using PANalytical SuperQ software. The PANalytical WROXI (wide-ranging oxides) calibration was used to determine the oxide concentrations in wt.%. The fused 40 mm beads used for measurements were made by mixing 10 g of lithium tetraborate (with 0.5%) flux with 1 g of sample. The specimen was heated in 5 steps before being poured and cooled: 1) 4 min at 1065℃ , 2) 3 min at 1065℃ rocking at 10 rpm and an angle of 15°, 3) 6 min at 1065℃ rocking at 30 rpm and an angle of 40°, 4) 1 min at 1000℃, 5) 4 min at 1000℃ rocking at 25 rpm and an angle of 45°. Measurements were taken in triplicates and the average values used.

The pH was measured to investigate sample pH evolution over time. A Mettler Toledo pH/Cond bench meter SE S470-K equipped with an expert proISM probe (error = ±0.01) was used to carry out all pH measurements; the probe was calibrated each day before use. The pH value at 0 day was measured right after mixing the cement paste; a small portion of the sample was separated, and the probe inserted into the paste directly. For the hardened samples, the pH was measured via the ex-situ leaching method (Behnood et al. 2016). A crushed powder sample of 1 g was added to 80 mL of distilled water (excess of solid material) and stirred with a magnetic stirrer. The pH reading was taken by inserting the testing probe into the solution, after 15 minutes of stirring to ensure that the measured solution was saturated and pH value became stable.

Thermogravimetric analysis (TGA) was also carried out to support the identification of species within the hardened cement that undergo thermal decomposition. Analysis was carried out on approximately 40 mg of sample in a PerkinElmer TGA 4000 heated from 30 ℃ to 990 ℃ at a heating rate of 10 ℃/min under a nitrogen flow of 40 mL/min; a 5 min isothermal hold was also appl ied at the start and end temperatures. A Hiden mass spectrometer (HPR-20 GIC EGA) was used to record the signals for H_2O, CO_2, O_2, CO, and H_2.

3. RESULTS AND DISCUSSION

3.1 M-S-H evolution: XRD

The XRD patterns of the samples with different initial water solutions are shown in Figures 2 a and b. According to the literature, amorphous broad humps at 10-13°, 20-30°, 35-39° and 58-6 2° 2θ stem from the produced M-S-H (Temuujin et al. 1998), and the broad hump at 18–25° 2θ represents the unreacted silica fume (Zhang et al. 2011). The brucite pattern consists of sharp peaks at approximately 18.6°, 38.0°, 50.8° and 58.6° 2θ (Temuujin et al. 1998). In the samples prepared with distilled water (Figure 2a), the intense peaks of brucite persist up to 56 days, indicating a slow consumption of brucite in this system. Accordingly, the formation of M-S-H appears to be slow, and peaks of M-S-H become apparent only at ≥ 28 days. A broad hump at 6-10° 2θ is slightly different from the expected range of 10-13° 2θ, but the increase in the peak intensity with the consumption of brucite suggests that this peak also represents M-S-H but in a slightly different from.

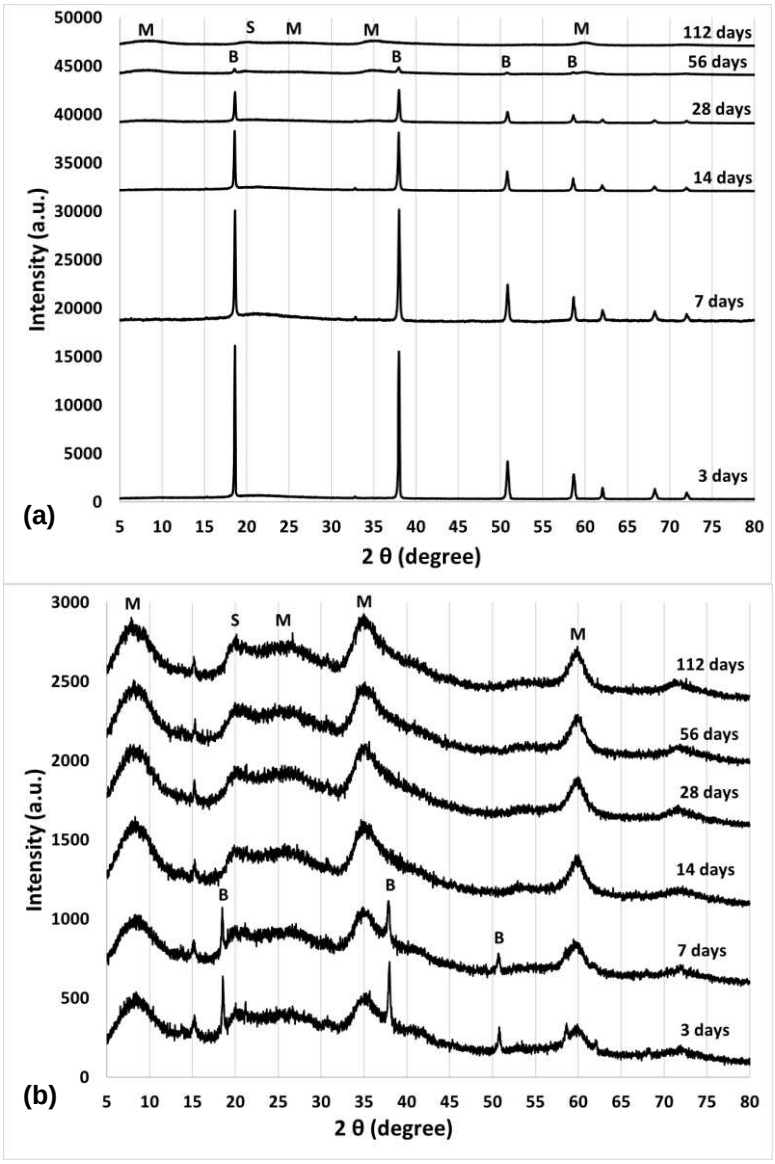

Figure 2. The XRD patterns showing the consumption of brucite (B) and silica fume (S), and the formation of M-S-H gel (M) over time in the samples prepared with: (a) distilled water and (b) $NaHCO_3$ solution.

The samples with $NaHCO_3$ addition (Figure 2b) showed much faster brucite reaction as the peaks of brucite disappeared within 14 days, while the M-S-H peaks can be clearly identified even after 3 days. The small peak observable at ~15° 2θ is likely to indicate the presence of hydromagnesite $Mg_5(CO_3)_4(OH)_2 \cdot 4H_2O$ (Suzuki et al. 2012). The consumption of silica fume is difficult to discuss in these samples due to the possible overlapping of the main hump at 18–25° 2θ with a M-S-H hump. At 112 days, both systems have similar XRD patterns with exception of small peaks of minor phases in $NaHCO_3$ containing systems. This indicates that M-S-H formation using distilled water sample has likely completed within 112 days. The addition of $NaHCO_3$ did not appear to significantly change the final M-S-H product. The XRD patterns clearly show that the M-S-H formation can be accelerated in the presence of $NaHCO_3$.

3.2 Mass balance: XRF

The oxide composition of the silica fume used in this work, derived through XRF analyses, and the loss on ignition (LOI) is shown in Table 3. Only oxides with >0.1 wt.% are presented in the Table. For the 100g of silica fume used, about 5.64g of other components are introduced into the sample. These impurities could be one of the reasons for the shift of the M-S-H hump at 10-13° 2θ to 6-10° 2θ observed in XRD data.

Table 3. Oxide composition of the silica fume

Element	SiO_2	K_2O	MgO	Fe_2O_3	Al_2O_3	Na_2O	CaO	ZnO	LOI
Weight %	94.36	1.12	0.71	0.61	0.50	0.32	0.22	0.20	1.82

XRF analyses was also carried out on the 56 day samples, and the results are shown in Table 4. Using these data, mass balance of the key elements was compared with the initial balance shown in Table 1, and the results are presented in Table 5. It is shown that the Mg/Si ratio in both samples remained approximately constant with small discrepancies probably arising from experimental error. This proves that the batch preparation was correct and that neither Mg nor Si were not lost in considerable amounts during washing with acetone. The Na/Mg ratios suggest that in the $NaHCO_3$ sample, the sodium remained in the sample, although the exact form of the sodium requires further investigation.

Table 4. The main element composition of the 56 days testing sample.

	MgO (wt.%)	SiO_2 (wt.%)	Na_2O (wt.%)
Distilled water	30.15	39.87	-
$NaHCO_3$	26.21	34.64	3.40

Table 5. Elemental mass ratio between the initial mixtures and 56 day cured samples.

	Initial (t=0)		t = 56 days	
	Mg/Si ratio	Na/Mg ratio	Mg/Si ratio	Na/Mg ratio
Distilled water	0.945	0.008	0.972	0.008
$NaHCO_3$	0.946	0.134	0.973	0.160

3.3 Progress of reaction: pH

The pH evolution for both sets of sample over 112 days is shown in Figure 3. The variation of the pH generally represents the change of the OH^- concentration in the solution. The dissolution of brucite will increase the pH of the solution, but only up to a maximum of ~10.5, which is the pH of saturated $Mg(OH)_2$ solution (Li et al. 2014). Therefore, in the $NaHCO_3$ samples, the pH values higher than 10.5 are likely due to the presence of alkaline element ions. The pH in this system decreases in the first 14 days and remains constant, consistent with pH evolution reported for similar systems (Li et al. 2014, Jin & Al-Tabbaa 2013), and can be attributed to the consumption of OH^- ions for the dissolution of silica and formation of $H_4SiO_4(aq)$, $[H_3SiO_4]^-$ and $[H_2SiO_4]^{2-}$ (Fertani-Gmati & Jemal 2011).

For the paste made with distilled water, pH was 9.48 at t = 0 and increased to 10.01 by 14 days; the pH then decreased slightly to 9.9 towards 112 days. In the first 14 days, the production of OH^- from the dissolution of $Mg(OH)_2$ appears more significant than the consumption of OH^- in the dissolution of SiO_2. After 14 days, these effects appear to be balanced. Since dissolution of $Mg(OH)_2$ should be continuing as the pH is below 10.5, this is likely due to the increased solubility of silica at a higher pH.

The $NaHCO_3$ sample had a relatively low pH value of 8.79 at day 0, which sharply increased to 10.59 by 3 days, then dropped to 10.22. The initial pH must be corresponding to that of the saturated $NaHCO_3$ solution (Table 1). The presence of $NaHCO_3$ clearly increased the pH of the mixture. The production of OH^- by dissolution of $Mg(OH)_2$ was much larger than the OH^- consumption rate in the first 3 days, but the high pH also encouraged the dissolution of silica and consumption of OH^-, resulting in the reduction of pH. The stable pH value after 14 days implies that majority of the reactions of the system, including M-S-H formation was completed, which is in agreement with XRD data.

The obtained results suggest that the availability of sodium and/or carbonate ions promote the reaction of $Mg(OH)_2$ and SiO_2, encouraging the M-S-H formation. Further research is required to elucidate the accelerated M-S-H development.

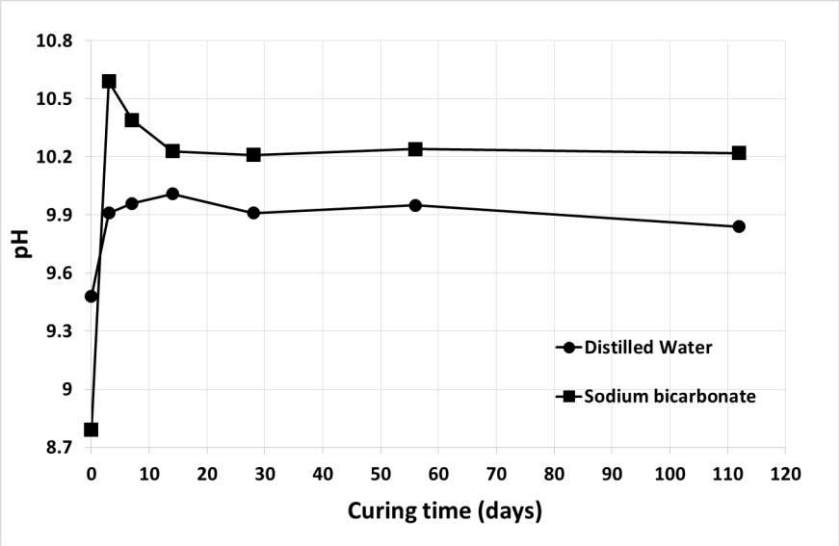

Figure 3. The results of pH test for all the samples

3.4 Development of phases: TGA

The differential thermogravimetric (DTG) curves obtained from TGA are shown in the Figure 4. For the samples with $NaHCO_3$ the 28 and 56 day samples were not tested as little progress of the reaction was suggested by XRD and pH data, but the 112 day samples were tested to compare the long-term behaviour.

The DTG peaks at 80-200 ℃ in the distilled water samples (Figure 4a) represent the loss of free water as well as water from M-S-H, while the decomposition of the brucite is represented by the peaks at around 400 ℃. The broad responses peaked at 500-600 ℃ are also caused by the loss of coordinated water in M-S-H (Jin & Al-Tabbaa 2013). It also clearly shows that, with the increase of curing time, the amount of M-S-H increased while the amount of $Mg(OH)_2$ decreased. This is an evidence of the continued consumption of brucite to form M-S-H. A minor discrepancy is observed between 3 day and 7 day data with regard to the amount brucite; but, as the variation is relatively small, this may be due to experimental error.

The $NaHCO_3$ sample (Figure 4b) indicated similar peaks associated with M-S-H and $Mg(OH)_2$; more M-S-H and less $Mg(OH)_2$ compared with the distilled water samples. The mass loss at around 450℃ in the $NaHCO_3$ sample may be explained by the presence of magnesite or hydromagnesite. Both of them are known to have TG responses at ~250 ℃ and 450 ℃ (Sheila 1993, Suzuki et al. 2012, Ren et al. 2014).

The $NaHCO_3$ samples have a fast reaction rate in the first 3 days as demonstrated from the amount of brucite remaining in the samples as well as the increased formation of M-S-H. The weight loss around 100℃ associated with M-S-H does not show a clear trend. This may be explained in three ways: (1) the presence of sodium and/or carbonate ions influenced the retention and bonding of molecular water in M-S-H, (2) this DTG peak also include the water loss from sodium carbonate hydrates or bicarbonate (Hartman et al. 2001), or (3) the experimental error associated with a small quantity of tested materials.

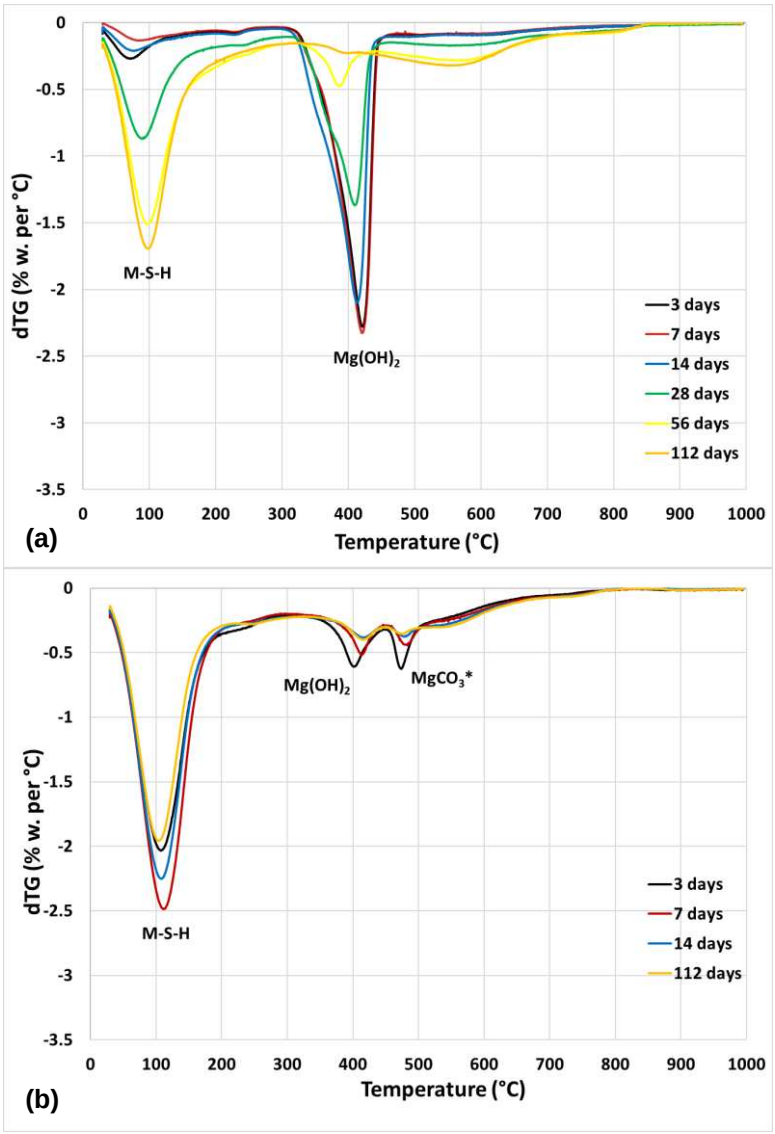

Figure 4. The DTG data obtained from TG analysis for: (a) distilled water sample and (b) $NaHCO_3$ samples. The symbol * implies possible contribution of these species.

4. CONCLUSION

The addition of $NaHCO_3$ promoted the reaction of $Mg(OH)_2$ and SiO_2 and resulted in the accelerated development of M-S-H gel. A higher pH of the mixing solution at ~10.2 appears to be beneficial to increase the dissolution of silica and formation of M-S-H. Further work is required to delineate these observations. Presence of carbonate ions in the system resulted in possible precipitation of hydromagnesite. The addition of $NaHCO_3$ also improved the fluidity of the paste and can allow for the production of magnesia-based concrete with a lower water/solid ratio without the addition of dispersants; thus, improving the strength. The availability of $NaHCO_3$ is also not foreseen an issue as sodium is one of the most abundant elements in the earth's crust. This work will reignite keen research interest into M-S-H cements.

5. REFERENCE

Behnood A., Van Tittelboom K. & De Belie N. (2016). Methods for measuring pH in concrete: A review. Construction and Building Materials 105: 176-188.

Fertani-Gmati M. & Jemal M. (2011). Thermochemistry and kinetics of silica dissolution in NaOH aqueous solution. Thermochimica Acta 513: 43-48.

Gartner E. & Sui T. (2018). Alternative cement clinkers. Cement and concrete Research 114: 27-39.

Hartman M., Trnka O., VeselÝ V. & Svoboda K. (2001). Thermal dehydration of the sodium carbonate hydrates. Chemical Engineering Communications 185 (1): 1-16.

Iler V.R.K. (1979). The Chemistry of Silica. Solubility, Polymerization, Colloid and Surface Properties, and Biochemistry. John Wiley and Sons.

Jin F. & Al-Tabbaa A. (2013). Thermogravimetric study on the hydration of reactive magnesia and silica mixture at room temperature. Thermochimica acta 566: 162-168.

Li Z., Zhang T., Hu J., Tang Y., Niu Y., Wei J. & Yu Q. (2014). Characterization of reaction products and reaction process of MgO-SiO_2-H_2O system at room temperature. Construction and Building Materials 61: 252-259.

Nied D., Enemark-Rasmussen K., L'Hopital E., Skibsted J. & Lothenbach B. (2016). Properties of magnesium silicate hydrates (MSH). Cement and Concrete Research 79: 323-332.

Ren H., Chen Z., Wu Y., Yang M., Chen J., Hu H., Liu J. (2014). Thermal characterization and kinetic analysis of nesquehonite, hydromagnesite, and brucite, using TG–DTG and DSC techniques. Journal of Thermal Analysis and Calorimetry 115: 1949–1960.

Sheila D. (1993). Thermal analysis studies on the decomposition of magnesite. International journal of mineral processing 37 (1-2): 73-88.

Suzuki Y., Suzuki T.S., Shinoda Y. & Yoshida K. (2012). Uniformly porous $MgTi_2O_5$ with narrow pore-size distribution: XAFS study, improved in situ synthesis, and new in situ surface coating. Advanced Engineering Materials 14 (12): 1134-1138.

Taylor M.G. & Collins D. (2006). Novel cements: low energy, low carbon cements. Fact Sheet 12.

Temuujin J., Okada K., & MacKenzie K.J.D. (1998). Role of Water in the Mechanochemical Reactions of MgO-SiO_2 Systems. Jouranl of Solid State Chemistry 138: 169-177.

Walling S.A., Kinoshita H., Bernal S.A., Collier N.C. & Provis J.L. (2015). Structure and properties of binder gels formed in the system $Mg(OH)_2$-SiO_2-H_2O for immobilisation of Magnox sludge. Dalton Transactions 44 (17): 8126-8137.

Walling S.A. & Provis J.L. (2016). Magnesia-based cements: a journey of 150 years, and cements for the future?. Chemical reviews 116 (7): 4170-4204.

Wang L., Chen L., Cho D-W., Tsang D.C.W., Yang J., Hou D., Baek K., Kua H.W. & Poon C-S. (2018). Novel synergy of Si-rich minerals and reactive MgO for stabilisation/solidification of contaminated sediment. Journal of hazardous materials 365: 695-706.

Zhang T., Cheeseman C.R. & Vandeperre L.J. (2011). Development of low pH cement systems forming magnesium silicate hydrate (MSH). Cement and concrete research 41 (4): 439-442.